# Prediction of a high-pressure phase transition and other properties of solid $CO_2$ at low temperatures

B. Kuchta* and R. D. Etters
*Physics Department, Colorado State University, Fort Collins, Colorado 80523*
(Received 9 March 1988)

An optimization procedure is used to minimize the Gibbs free energy of solid $CO_2$ at pressures $0 \leq P \leq 16$ GPa, with respect to the unit-cell parameters, center-of-mass coordinates, and orientations of all the independent molecules. A lattice-dynamics procedure is used to calculate the libron frequencies. The observed *Pa*3 structure is predicted at low pressures, and a transition to an orthorhombic *Cmca* phase is found at $P=4.3$ GPa, with a volume change $\Delta V=0.3$ cm$^3$/mole. The calculated second virial coefficients, sublimation energy, molar volume, pressure-volume relation, and libron frequencies in the *Pa*3 phase are in good agreement with experiment. In the *Cmca* phase the calculated libron frequencies agree fairly well with recent Raman scattering results. An analysis of the potential-energy surface shows that the large observed hysteresis associated with the transition may be the result of large barriers between the phases.

## I. INTRODUCTION

The cubic *Pa*3 structure of solid $CO_2$, shown in Fig. 1(a), is the only known solid phase.[1,2] This is because the large quadrupole moment of the $CO_2$ molecule stabilizes this phase to much higher temperatures and pressures than in crystals like $N_2$ and CO, which also exhibit other solid phases. Recent Raman spectra at room temperature[3] have shown evidence of a new phase at $P \simeq 18$ GPa, and indications of another phase were found at pressures $0.5 \leq P \leq 2.3$ GPa by Liu.[4,5] Other Raman[3] and x-ray measurements[2] found no evidence of this low-pressure phase.

More recent Raman scattering results[6] confirm the earlier room-temperature results at 18 GPa and, at temperature $T=40$ and 80 K, there is clear evidence of what is probably the same transition at $P=11\pm2.5$ GPa. However, a very large hysteresis was observed. When unloading at 80 K, $CO_2$ transformed back to the cubic *Pa*3 phase only at $2.5 \leq P \leq 4.5$ GPa. Additionally, peaks that appear associated with the libron modes of the *Pa*3 phase were found at pressures well above the quoted transition at $P=11$ GPa, and modes that appear associated with the new high-pressure phase were found well below the transition pressure, although in both cases the results were not reproducible but instead depended upon the history of the sample and the way in which the measurements were taken. Compounding the problem of interpreting the experimental data is the observation that large pressure gradients exist across the sample that increase with increasing pressure. This increases the possibility of uniaxial stress. Nevertheless, three Raman lines could clearly be distinguished, identifying the new phase. It was conjectured[6] that the strongest of these lines, which is fairly broad, is in fact two separately unresolved lines. The measured[6] vibron lines appear insensitive to the transition.

We have examined three previous calculations, that used different models[7-9] for the $CO_2$-$CO_2$ potential, which gave reasonable predictions for certain properties of the *Pa*3 phase at zero pressure. However, our calculations of other properties showed that each of these potential models are inadequate. Gibbons and Klein[10] performed extensive calculations of thermodynamic quantities over a range of temperatures using a previously formulated Lennard-Jones 6-12 potential that was also modified to improve certain results. A 6-9 expression was also used. We did not explore these potentials because the unphysical repulsive parts would certainly be unsatisfactory at high pressures. Consequently, we have constructed a new semiempirical expression for the interactions that has been used to calculate a wide variety of properties both at zero and high pressures.

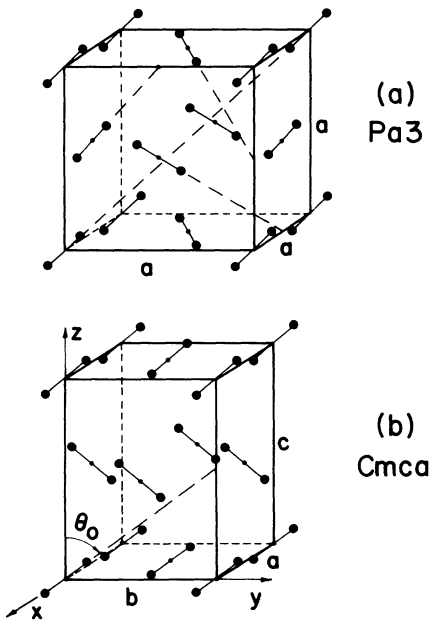


FIG. 1. The cubic *Pa*3 and orthorhombic *Cmca* structures are shown an the lattice constants *a*,*b*, and *c* are identified. A Cartesian reference frame is also shown.

 

## II. THE POTENTIAL AND METHOD

The repulsive overlap and attractive dispersion interactions between two $CO_2$ molecules are given by a site-site expression. The three force centers (sites) on each molecule are located on the carbon atom and at positions $l=\pm 1.06$ Å away from the center, which we identify as the C site and O sites, respectively. It is noted that the 0 sites, however, are not located on the oxygen atoms but somewhat interior to them. In this calculation the bond length of the molecule is assumed to be fixed at $d=2.32$ Å. The three curves in Fig. 2 show the interaction between the O-O, O-C, and C-C sites, respectively, which were numerically tabulated. Intermediate values were determined using a quadratic interpolation formula. Analytic expressions will be formulated in a forthcoming article. The electric quadrupole moment is taken to be[11] $\Theta=-4.3\times10^{-26}$ esu cm$^2$, and the hexadecapole is $\Phi=-1.85\times10^{-26}$ esu cm$^4$, which is near the value reported by Murthy *et al.*[8] These multipoles are simulated by placing point charges (1.04, −2.08, 1.04), in units of the electron charge, at positions 0.656 Å, 0.0 Å, and −0.656 Å, respectively, along each molecular axis. The origin is located on the carbon atom. The multipole interactions are then determined by summing the Coulomb interactions between the charges on different molecules.

The structures are determined at each pressure along the zero-temperature isotherm by minimizing the Gibbs free energy $G$. Crystallographic unit cells containing three or four independent molecules were examined where all molecular mass centers, orientations, and the cell parameters were independently varied in the minimization process. Upon determining the structures and molar volumes at each pressure, the zone-center libron frequencies were calculated using a lattice-dynamics procedure. Discrete lattice sums were taken out to 9 Å and a continuum correction was made for larger separations.

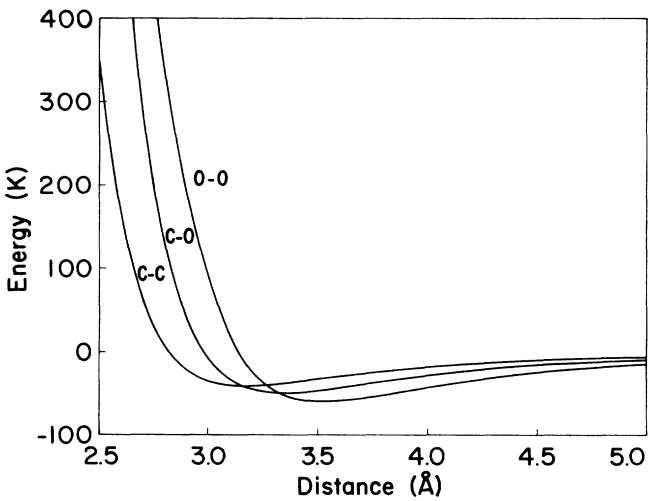


FIG. 2. The repulsive overlap and dispersion interactions between the O-O and C-O, and C-C sites on different molecules.

## III. RESULTS

The solid line in Fig. 3 shows the second virial coefficients calculated using the potential shown in Fig. 2, and the solid circles represent the experimental data.[12] This agreement is a major improvement over results obtained using previously developed potentials,[7-9] and it depends strongly on the location and magnitude of the charges used to simulate quadrupole and hexadecapole moments.

At zero pressure and temperature the system stabilizes into the cubic $Pa3$ phase and the calculated volume and sublimation energy are 25.6 cm$^3$/mole and −3243 K, which compare quite favorably with the experimental values.[1,13,14] The solid line in Fig. 4 gives the calculated zero-temperature pressure-volume relation and a phase transition to a *Cmca* orthorhombic structure, shown in Fig. 1(b), is observed at $P=4.3$ GPa, with a volume change on transition of $\Delta V=0.3$ cm$^3$/mole. It is characterized by a crossing of the zero-temperature Gibbs free energy for the two structures. The transition region is shown in more detail in the inset. The dashed line gives the $P$-$V$ curve at higher pressures where the system has been constrained to the $Pa3$ phase. This curve and the extension of it for this phase at lower pressures agrees very closely with recent results, calculated at zero temperature using electron-gas methods.[15] The solid circles represent room-temperature measurements for the $Pa3$ structure[2] and applying thermal corrections to our zero-temperature curve[15] brings the two into good agreement, as is evidenced by the merging to the dashed line with the solid circles at high pressure, where thermal corrections are relatively small. The diamond represents the measured value of the volume[13] at zero pressure and low temperatures.

The open diamonds, squares, and triangles in Fig. 5 give the observed[6] libron frequencies at low temperatures versus pressure for the $Pa3$ phase and the dashed lines give our calculated results. The open circles along these curves are measured values[6] which appear in the spectra associated with the new high-pressure phase, and that they fit nicely as extensions of the $Pa3$ spectra is reveal-

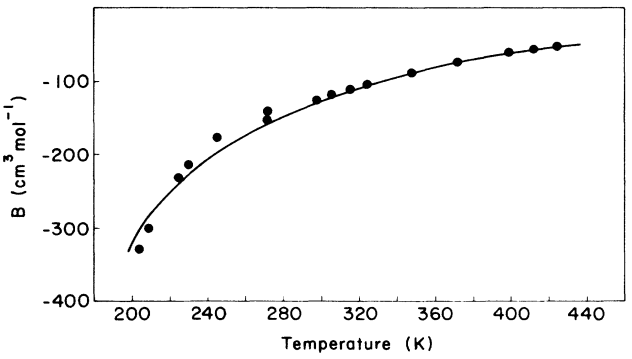


FIG. 3. The solid line gives the calculated second virial coefficients and the solid circles are the experimental data (Ref. 12).

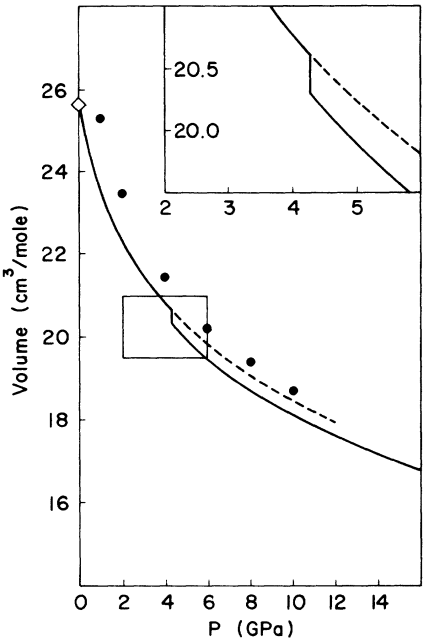


FIG. 4. The solid lines give the calculated zero temperature $P$-$V$ curve, and the dashed line is the extension of the curve for $P > 4.3$ GPa with the system constrained to the $Pa3$ structure. The solid circles are experimental results at room temperature (Ref. 2) and the diamond is the measured volume at low temperature (Ref. 13).

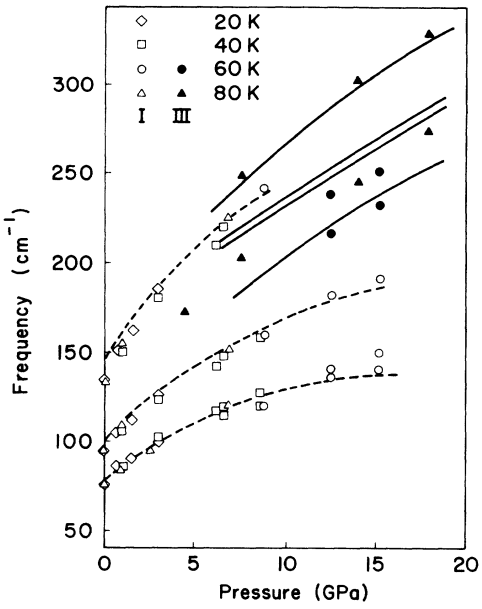


FIG. 5. The open diamonds, squares, and triangles give the measured libron frequencies (Ref. 6) in the $Pa3$ phase at low temperatures, and the dashed lines are the calculated values. The open circles along these curves are measured Raman peaks in the region associated with the high-pressure phase. The solid triangles and circles are the measured frequencies in the high-pressure phase and the solid lines are calculated values.

ing. The solid triangles and circles at higher frequencies and pressures show the three observed modes[6] of the new phase and the solid lines represent our calculations for the predicted orthorhombic structure. The middle two calculated lines are close to the measured peak that has been suggested[6] is an unresolved double peak.

Table I gives the calculated Gibbs energy and lattice parameters for the $Pa3$ and $Cmca$ phases versus pressure.

## IV. DISCUSSION AND CONCLUSIONS

The calculated second virial coefficient and the zero-pressure solid structure, molar volume, sublimation energy, and zone-center libron frequencies are in remarkably good agreement with experiment. Moreover, the agreement of the calculated libon frequencies with experiment for the high-pressure phase supports our prediction that

TABLE I. Lattice parameters and Gibbs free energies ($T = 0$ K) of $Pa3$ and $Cmca$ structures of solid $CO_2$. The calculated uncertainty in the parameters $a$, $b$, and $c$ is $\pm 0.05$ Å, and it is $\pm 0.5°$ in the polar angle $\theta_0$, defined in Fig. 1(b).

| | $Pa3$ | | $Cmca$ | | | | |
|---|---|---|---|---|---|---|---|
| $P$ (GPa) | $a$ (Å) | $G$ (K) | $a$ (Å) | $b$ (Å) | $c$ (Å) | $\theta_0$ (deg) | $G$ (K) |
| 0 | 5.54 | −3243 | 4.85 | 5.37 | 6.53 | 52.3 | −3090 |
| 2.8 | 5.23 | 4591 | 4.50 | 5.00 | 6.29 | 52.2 | 4652 |
| 3.2 | 5.20 | 5622 | 4.47 | 4.94 | 6.28 | 52.2 | 5656 |
| 3.4 | 5.19 | 6132 | 4.46 | 4.94 | 6.26 | 52.1 | 6159 |
| 3.8 | 5.17 | 7143 | 4.44 | 4.93 | 6.24 | 52.1 | 7158 |
| 4 | 5.16 | 7645 | 4.44 | 4.92 | 6.23 | 52.1 | 7652 |
| 4.2 | 5.15 | 8143 | 4.43 | 4.91 | 6.22 | 52.0 | 8145 |
| 4.4 | 5.15 | 8639 | 4.42 | 4.90 | 6.21 | 52.0 | 8635 |
| 4.6 | 5.14 | 9133 | 4.35 | 4.90 | 6.24 | 52.0 | 9112 |
| 4.8 | 5.13 | 9623 | 4.35 | 4.89 | 6.23 | 52.0 | 9595 |
| 5.2 | 5.11 | 10 598 | 4.33 | 4.88 | 6.22 | 52.0 | 10 554 |
| 5.6 | 5.10 | 11 564 | 4.31 | 4.86 | 6.21 | 52.0 | 11504 |
| 8 | 5.02 | 17 202 | 4.27 | 4.75 | 6.10 | 51.9 | 17 016 |
| 12 | 4.92 | 26 119 | 4.17 | 4.65 | 6.02 | 51.9 | 25 733 |

it forms an orthorhombic *Cmca* structure, exactly like the ground state of the halogens[16] $Cl_2$, $Br_2$, and $I_2$. Acetylene also exhibits[17,18] a *Pa*3 to *Cmca* transition at $T=133$ K, under zero pressure, and at $P=9$ kbar at 300 K. Unlike $CO_2$ there is no observed hysteresis. The ability of the unit cell to arbitrarily deform from its assumed initial state, during the minimization procedure, virtually eliminates any *a priori* bias in the outcome of the predicted structure at any pressure, although some care had to be taken in choosing the initial conditions in the optimization because large potential barriers inhibiting the transition between phases developed at high pressures. As a consequence the system occasionally evolved into a metastable state rather than the ground state. For that reason it was always necessary to monitor the Gibbs free energy. As will be discussed shortly, these barriers may account for the large experimentally observed hysterisis.[6] All calculations based upon four independent molecules per unit cell spontaneously reduced to two molecule unit cells. Unit cells containing three molecules exhibited no stable configurations. Occasionally a two molecule per tetragonal unit cell, isomorphic with the $P4_2/mnm\gamma$-$N_2$ phase would stabilize but, in all cases, an examination of the Gibbs free energy revealed it was only metastable and not the equilibrium state of the system.

The predicted phase transition pressure $P=4.3$ GPa is between the limits observed[6] upon loading and unloading $2.5<P<11$ GPa, and it is therefore reasonable. In order to understand the large hysteresis associated with the transition between the *Cmca* and *Pa*3 structures, the energy surface corresponding to a molecular rotation through an azimuthal angle $\varphi$ associated with the *Pa*3 orientations, see Fig. 1, to an orientation along the *bc* plane, as in the *Cmca* structure, was mapped. The polar angle $\theta$ was found to change very little through the transition. A plot of the Gibbs free energy versus $\varphi$ at $P=0$ showed a minimum only for the *Pa*3 structure but, with increasing pressure a minimum occurred for $\varphi$ associated with the *Cmca* structure that became equally deep with *Pa*3 at $P=4.3$ GPa. These two minima are separated by a barrier 225 K high. As $P$ increases further, the well associated with the *Cmca* structure gets deeper but the barrier height above the *Pa*3 minimum remains the same, only its width diminishes. The following scenario may at least partially explain the hysteresis. Upon loading at low temperatures the barrier cannot be breached until $G(Cmca)$ is much lower than $G(Pa3)$, where the width of the barrier is substantially reduced. Upon unloading from the *Cmca* phase as $P\geq 11$ GPa, the barrier that must be overcome in the transition to *Pa*3 is very high, and does not reduce to 225 K until $P=4.3$ GPa. As with loading this is still too high and $P$ must be reduced considerably more before the barrier is sufficiently small to initiate the transition. While this is an oversimplified argument, it may be an essential element in understanding the experimental results. If so, one should expect much smaller hysteresis at room temperature, which remains to be examined.

Our calculated results, based upon previously developed potentials, gave a variety of predictions for the high-pressure phases of $CO_2$, including *Pa*3, orthorhombic, tetragonal, or both orthorhombic and tetragonal. It was generally observed that reducing the distance between the C and O force centers raised the orthorhombic transition pressure and increasing the hexadecapole moment favored the stability of the tetragonal phase with respect to the orthorhombic phase at high pressures. Because of the uncertainties in the potential it must be admitted that the tetragonal structure cannot be rules out as a possible high-pressure phase. However, there are two features of the tetragonal phase that make it improbable as the physically realized state. First of all, there are only two Raman active modes, instead of the three or possibly four experimentally observed,[6] and our calculations of these frequencies do not agree well with those measured. Secondly, the potential barrier that must be overcome in transition from *Pa*3 to this phase is exceedingly large and it is therefore not likely to be realized. Consequently, we believe that the *Cmca* phase is overwhelmingly the most plausible.

## ACKNOWLEDGMENTS

We wish to thank the CSU University Computer Center for providing time on the CDC Cyber 205 computer within the CSU Supercomputing Project. This work was supported by U.S. Department of Energy (DOE) Contract No. DE-FG02-86ER45238.

*Permanent address: Institute of Organic and Physical Chemistry, Technical University of Wroclaw, 50-370 Wroclaw, Poland.

[1]W. H. Keesom and J. W. L. Kohler, Physica **1**, 655 (1934); A. E. Curzon, Physica **59**, 733 (1972).
[2]B. Olinger, J. Chem. Phys. **77**, 6255 (1982).
[3]R. C. Hanson, J. Phys. Chem. **89**, 4499 (1985).
[4]L. Liu, Earth Planet Sci. Lett. **71**, 104 (1984).
[5]L. Liu, Nature (London) **303**, 508 (1983).
[6]H. Olijnyk, H. Daufer, H.-J. Jodl, and H. D. Hochheimer (unpublished).
[7]A. I. Kitaigorodski, K. V. Mirskaya, and V. V. Nauchitel, Kristallografiya **14**, 900 (1969) [Sov. Phys.—Crystallogr. **14**, 769 (1970)].
[8]C. S. Murthy, S. F. O'Shea, and I. R. McDonald, Mol. Phys. **50**, 531 (1983).
[9]P. Procacci, R. Righini, and S. Califano, Chem. Phys. **116**, 171 (1987).
[10]T. G. Gibbons and M. L. Klein, J. Chem. Phys. **60**, 112 (1974).
[11]A. D. Buckingham, R. L. Disch, Proc. R. Soc. London, Ser. A **273**, 275 (1963).
[12]J. H. Dymond and E. B. Smith, *The Virial Coefficients of Gases* (Clarendon, Oxford, 1969).
[13]V. G. Manzheli, A. M. Tolkuchev, M. I. Bagatskii, and E. I. Vostovich, Phys. Status Solidi B **44**, 39 (1971).
[14]J. A. Pople, Proc. R. Soc. London, Ser. A **221**, 508 (1954).

[15]R. LeSar and R. G. Gordon, J. Chem. Phys. **78**, 4991 (1983).
[16]K. Takemura, S. Minomura, O. Shimomura, and Y. Fijii, Phys. Rev. B **26**, 998 (1982); E. D. Stevens, Mol. Phys. **37**, 27 (1979); B. Vonnegut and E. B. Warren, J. Am. Chem. Soc. **58**, 2459 (1936).
[17]K. Aoki, Y. Kakudate, M. Yoshida, S. Usuba, K. Tanaka, and S. Fujiwara, Solid State Commun. **64**, 1329 (1987).
[18]R. LeSar, J. Chem. Phys. **86**, 1485 (1987).